Excitation strengths in ^{109}Sn: Single-neutron and collective excitations near ^{100}Sn

D. D. DiJulio,[1,*] J. Cederkall,[1] C. Fahlander,[1] A. Ekström,[2] M. Hjorth-Jensen,[2,3] M. Albers,[4,†] V. Bildstein,[5,‡] A. Blazhev,[4]
I. Darby,[6] T. Davinson,[7] H. De Witte,[6] J. Diriken,[6,8] Ch. Fransen,[4] K. Geibel,[4] R. Gernhäuser,[5] A. Görgen,[9] H. Hess,[4]
J. Iwanicki,[10] R. Lutter,[11] P. Reiter,[4] M. Scheck,[12,§] M. Seidlitz,[4] S. Siem,[9] J. Taprogge,[4] G. M. Tveten,[9] J. Van de Walle,[13]
D. Voulot,[14] N. Warr,[4] F. Wenander,[14] and K. Wimmer[5,‖]

[1]*Physics Department, Lund University, Box 118, SE-221 00 Lund, Sweden*
[2]*Department of Physics and Center of Mathematics for Applications, University of Oslo, N-0316, Oslo, Norway*
[3]*National Superconducting Cyclotron Laboratory and Department of Physics and Astronomy,*
Michigan State University, East Lansing, Michigan 48824, USA
[4]*Institute of Nuclear Physics, University of Cologne, Germany, D-50937 Cologne, Germany*
[5]*Physik Department E12, Technische Universität München, D-85748 Garching, Germany*
[6]*Instituut voor Kern- en Stralingsfysica, KU Leuven, Celestijnenlaan 200D, B-3001 Leuven, Belgium*
[7]*Department of Physics and Astronomy, University of Edinburgh, Edinburgh, United Kingdom*
[8]*Studiecentrum voor Kernenergie/Centre d'Etude de l'énergie Nucléaire (SCK CEN), B-2400 Mol, Belgium*
[9]*Department of Physics, University of Oslo, Oslo, Norway*
[10]*Heavy Ion Laboratory, University of Warsaw, Warsaw, Poland*
[11]*Fakultät für Physik, Ludwig-Maximilians-Universität München, D-85748 Garching, Germany*
[12]*Oliver Lodge Laboratory, University of Liverpool, Liverpool, United Kingdom*
[13]*PH Department, CERN 1211, Geneva 23, Switzerland*
[14]*AB Department, CERN 1211, Geneva 23, Switzerland*

A set of $B(E2)$ values for the low-lying excited states in the radioactive isotope ^{109}Sn were deduced from a Coulomb excitation experiment. The 2.87-MeV/u radioactive beam was produced at the REX-ISOLDE facility at CERN and was incident on a secondary ^{58}Ni target. The $B(E2)$ values were determined using the known $2^+ \rightarrow 0^+$ reduced transition probability in ^{58}Ni as normalization with the semiclassical Coulomb excitation code GOSIA2. The transition probabilities are compared to shell-model calculations based on a realistic nucleon-nucleon interaction and the predictions of a simple core-excitation model. This measurement represents the first determination of multiple $B(E2)$ values in a light Sn nucleus using the Coulomb excitation technique with low-energy radioactive beams. The results provide constraints for the single-neutron states relative to ^{100}Sn and also indicate the importance of both single-neutron and collective excitations in the light Sn isotopes.

We report here on measurements using Coulomb excitation of the nucleus ^{109}Sn, with the aim of investigating the nature of the low-lying excited states in this nucleus. Of particular interest is the location of the single-neutron states, which provide important constraints for shell-model calculations. For the light Sn isotopes, these include the $g_{7/2}$, $d_{5/2}$, $s_{1/2}$, $d_{3/2}$, and $h_{11/2}$ single-neutron orbits. Only a limited number of studies have been reported using Coulomb excitation in the odd-Sn isotopes. In earlier work, the technique was used to investigate the collectivity of excited states in ^{115,117,119}Sn [1,2]. More recently, we reported on the first Coulomb excitation measurement in the isotope ^{107}Sn [3]. That measurement

resulted in an enhanced reduced transition probability in comparison to shell-model calculations, which indicates the importance of mixing between single-neutron and collective excitations near the doubly magic nucleus ^{100}Sn. In addition, in a series of recent measurements, Coulomb excitation was used to determine the reduced transition probabilities of the first 2^+ states in the neutron-deficient Sn isotopes ^{106,108,110}Sn [4–7]. Also there the reduced transition probabilities were increased by ∼30% with respect to state-of-the-art shell-model calculations based on realistic nucleon-nucleon interactions.

The experimentally known systematics for the single-neutron states in the odd-Sn nuclei are highlighted in Fig. 1 [8]. In ^{111}Sn, these states have been firmly identified in previous reaction studies [9]. However, similar data are not available for the lighter nuclei and the current information is based on a number of different measurements, comparison to theory, and systematic trends. Down to ^{103}Sn, the ground-state and first excited-state spins are believed to be $5/2^+$ and $7/2^+$, respectively. Recently, the energy splitting between these two levels in ^{101}Sn has been reported in two different measurements as 172 keV [10,11]. The energy splitting is similar to the 168-keV difference in ^{103}Sn [12]. Based on the energy systematics alone, this favors a $5/2^+$ ground state and a

---

*douglas.dijulio@nuclear.lu.se
†Present address: Physics Division, Argonne National Laboratory, Argonne, Illinois 60439, USA.
‡Present address: Department of Physics, University of Guelph, Guelph, Ontario NIG 2W1, Canada.
§Present address: Institut für Kernphysik, Technische Universität Darmstadt, D-64289 Darmstadt, Germany.
‖Present address: National Superconducting Cyclotron Laboratory. Michigan State University, East Lansing, Michigan 48824, USA.
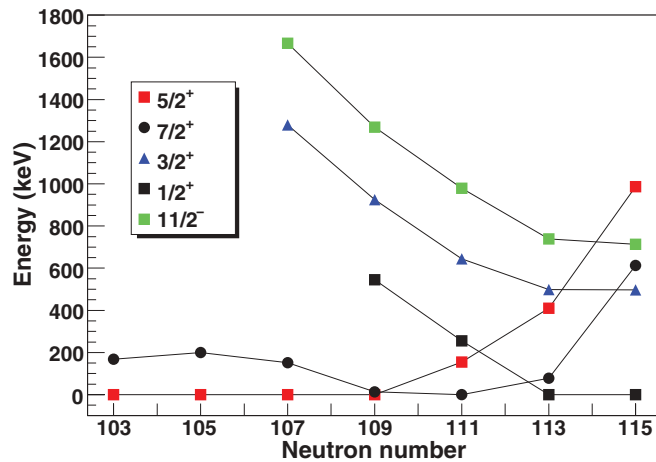
FIG. 1. (Color online) The experimental single-neutron states in the neutron-deficient Sn nuclei, using energies given in Ref. [8].

$7/2^+$ first excited state. However, measurements in Ref. [11] indicated that the level ordering is instead inverted with respect to ^{103}Sn. This could be the result of a strong pairing interaction between neutrons in the $g_{7/2}$ orbit. Shell-model calculations do not provide any further information as both lowest-lying orbits result in the correct ordering of the $5/2^+$ and $7/2^+$ states in the light Sn nuclei. The spin ordering of the two states in ^{101}Sn thus remains an open question.

In ^{109}Sn, the ground-state spin has been measured to be $J = 5/2$ in a hyperfine splitting experiment [13], possibly corresponding to a single neutron in the $d_{5/2}$ neutron orbit. The first excited $7/2^+$ level, lying at 13 keV above the ground state, is believed to be the $g_{7/2}$ single-neutron state [14], while a level at 925 keV has been suggested to be the $d_{3/2}$ state based on the β-decay feeding strength [15,16]. The level at 545 keV is thought to be the $s_{1/2}$ state also based on β-decay measurements. The state was, however, previously suggested to have a spin and parity of $3/2^+$ [15].

In addition to states of single-neutron character, we might also expect to observe states originating from the coupling of a particle or hole to a core state in a neighboring even-even Sn isotope [17]. These excitations are expected to have larger $B(E2)$ values than the single-neutron states. Any mixing between these types of excitations may, however, affect the electromagnetic properties of the states. In the Coulomb excitation of the nuclei ^{117,119}Sn, two $3/2^+$ states exhibited properties that were good examples of single-neutron and collective excitations [1]. Here, we aim to extend this type of investigation to the nucleus ^{109}Sn.

The ^{109}Sn radioactive beam was produced at the REX-ISOLDE facility at CERN. The method has been described in detail in a number of previous publications [3,5,7] and is presented only briefly here. The isobaric beam was produced by reactions in a 27-g/cm^2 LaC$_x$ target induced by a 1.4-GeV proton beam with a maximum intensity of $\sim 3 \times 10^{13}$ protons per pulse (typically 9 pulses/min), ionization using a resonant laser ionization scheme [18], and separation according to $A = 109$ in the general purpose separator. The radioactive beam, consisting of Sn and In, was accelerated to an energy of 2.87 MeV/u before bombarding the 99.93%

isotopically enriched ^{58}Ni secondary target. The beam purity was calculated to be 89(1)% from the number of particles collected in a double-sided silicon strip detector (DSSSD) placed downstream of the secondary target [19] from the laser-on and laser-off runs. The Sn beam was estimated to have an intensity of $\sim 10^5$ particles per second.

Following Coulomb excitation in the secondary target, the emitted γ rays were identified using the MINIBALL γ-ray detector array [20]. The Ge clusters of the array were positioned around the target. The DSSSD was used to identify the scattered beam and target particles. The DSSSD contained four separate quadrants. Each consisted of 16 annular strips and 24 pairwise coupled radial strips. The results presented in this work were obtained by implementing the following conditions on the data: (1) building particle events based on a single front and back strip hit in the DSSSD; (2) selection of events in which one particle ($1p$) or two particles ($2p$) were detected; (3) applying a $2p$ time cut and requiring that the two particles were detected in opposite quadrants of the DSSSD; (4) identification of Sn and Ni particles through implementation of a kinematical cut; (5) reconstruction of the missing particles in the $1p$ data set; and (6) imposing a time coincidence condition between the particles and γ rays and subsequent event-by-event Doppler correction of the resulting γ-ray spectrum. The last condition is required as γ rays from the scattered beam and projectile particles are emitted in flight.

The Doppler-corrected spectra gated on Ni and Sn particles collected in the DSSSD are shown in panels (a) and (b) of Fig. 2, respectively. The data correspond to Ni particles collected in the angular range of 28.9–49.3°. A single peak, resulting from the $2^+ \to 0^+$ transition in ^{58}Ni at 1454 keV, is seen in the Ni spectrum [21]. This state has an adopted reduced transition probability of $B(E2; 0^+ \to 2^+) = 0.0704(15)$ e^2b^2 [21], which is used in the analysis described below. In the Sn spectrum, several previously known transitions are observed [22]. The extracted peak areas and relative intensities are given in Table I and the adopted level scheme for ^{109}Sn is presented in Fig. 3 [22]. The peak around 664 keV is a combination of both the $3/2_1^+ \to 5/2_1^+$ and $5/2_2^+ \to 7/2_1^+$ transitions. Furthermore, it was not possible to resolve the 678-keV $5/2_2^+ \to 5/2_1^+$ transition. In the analysis, a fit consisting of two Gaussian

TABLE I. Measured peak areas and relative intensities from the Coulomb excitation experiment. Energies given in Refs. [16,21,22].

Transition	E_γ (keV)	Area	Rel. int.
Sn $3/2_1^+ \to 5/2_1^+$ / $5/2_2^+ \to 7/2_1^+$	665/664	462(40)	0.82(8)
Sn $5/2_2^+ \to 5/2_1^+$	678	60(31)	0.11(6)
Sn $3/2_2^+ \to 5/2_1^+$	925	277(32)	0.60(7)
Sn $1/2_2^+ \to 5/2_1^+$	991	99(26)	0.22(6)
Sn $7/2_2^+ \to 5/2_1^+$ / $7/2_2^+ \to 7/2_1^+$	1078/1064	390(37)[a]	0.93(10)[a]
Sn $9/2_1^+ \to 5/2_1^+$	1240	278(27)	0.72(8)
Ni $2^+ \to 0^+$	1454	350(30)[b]	1.00(9)[b]

[a]May also contain a contribution from the $3/2_3^+ \to 5/2_1^+$ transition at 1062 keV.

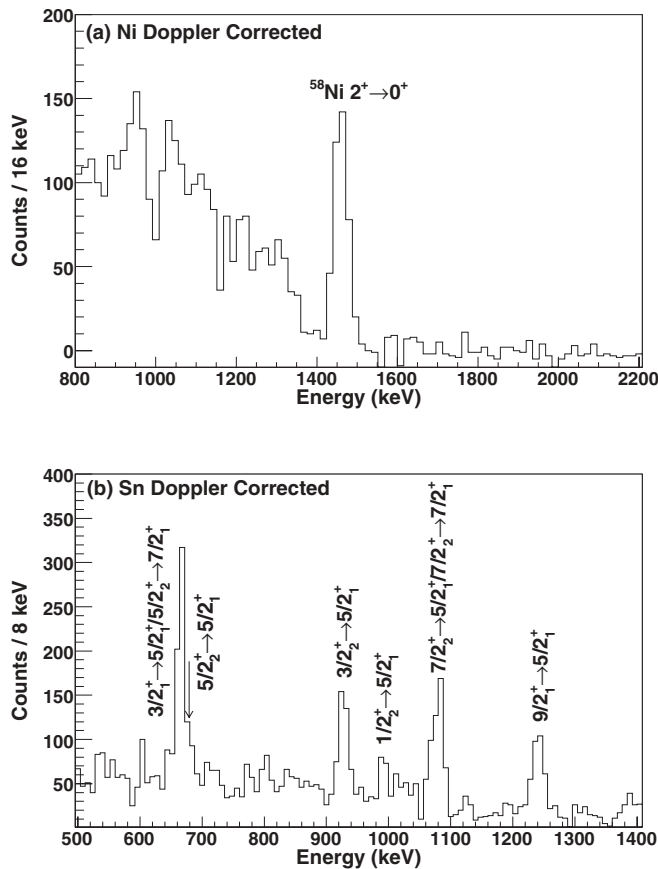[b]Calculated from the Ni peak area in Fig. 2(a) and the beam purity given in the text.

FIG. 2. The Doppler corrected γ-ray spectra gated on (a) Ni and (b) Sn particles. The spectra have been corrected for random background coincidences. The labels indicate the transitions used in the analysis.

FIG. 3. The experimentally known level scheme (Exp) for ^{109}Sn and the shell-model (SM) calculated energy levels [16,22]. See text for details of the shell-model calculation.

peaks was used to extract areas for the 664-keV doublet and the 678-keV transition. The peak at 1078 keV may be a triplet related to the 1078-keV $7/2_2^+ \rightarrow 5/2_1^+$, 1064-keV $7/2_2^+ \rightarrow 7/2_1^+$, and 1062-keV $3/2_3^+ \rightarrow 5/2_1^+$ transitions. The weight of the peak is close to 1078 keV, suggesting that it is predominantly related to the $7/2_2^+ \rightarrow 5/2_1^+$ transition. In Ref. [15], the $7/2_2^+ \rightarrow 7/2_1^+$ transition was measured to be 22% of the intensity of the transition to the ground state. The peak area in Table I is therefore given as doublet containing these two contributions. The known branching ratios for the 678- and 1078-keV states were included in the analysis discussed below. The 991-keV level was not directly fed in previous β-decay experiments nor does it feed the 14-keV $7/2^+$ state [16]. Based on these arguments, a spin of $1/2^+$ was adopted for this level.

The experimentally determined yields have been analyzed with the semiclassical Coulomb excitation code GOSIA2 [23] to determine a set of reduced transition probabilities for the observed excited states. The code uses a χ^2 minimization routine to reproduce the experimentally measured yields, treating the reduced matrix elements as free parameters and using the known ^{58}Ni matrix elements as normalization. The input to the code requires a set of excited states, starting values for the reduced matrix elements connecting the states, the geometry of the particle and γ-ray detectors, and in addition
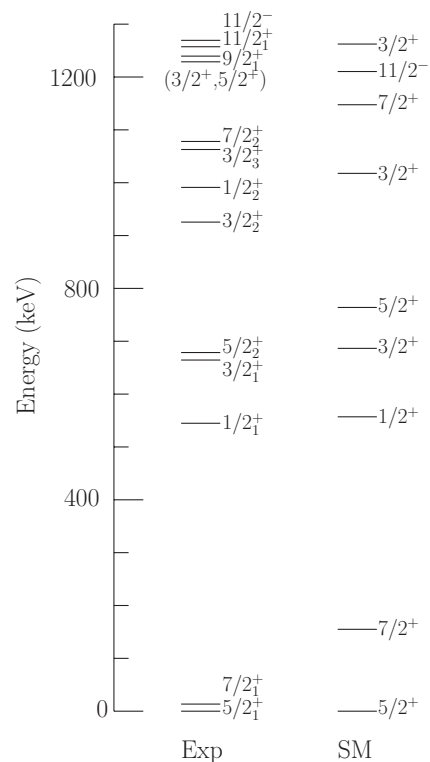
any previously known experimental data such as branching ratios, lifetimes, and mixing ratios. Corrections for energy loss in the target, internal conversion coefficients, and the angular distribution of the emitted γ rays are accounted for by the code.

In the analysis, ten excited states were included, corresponding to the observed levels, and two additional higher lying states to account for any unobserved excitation. The population of these states is dominated by the $E2$ reduced matrix elements while both the $E2$ and $M1$ matrix elements are important for the decay of the states. All $E2$ and $M1$ reduced matrix elements coupling the ten states were included in the analysis. The starting values have been taken from shell-model calculations, discussed below. The known spectroscopic quadrupole moment of the ground state, measured in a hyperfine splitting experiment, was used instead of the shell-model value in the analysis [13].

During the fit, fifteen $E2$ and $M1$ matrix elements important for the reproduction of fifteen data points, including the measured yields and nine previously known branching ratios [16,22], were varied. The remaining matrix elements were fixed in the analysis. The determined transition probabilities are given in Table II. The errors were estimated by fixing each individual transition probability to points around the minimum. At each point, the fit was repeated while the Ni matrix elements were free to vary between their 1σ limits along with the remaining unfixed Sn matrix elements. This procedure was carried out until the $\chi^2 + 1$ limit was determined. Each $E2$ transition was also fit individually with all other matrix elements set to zero. The effects are included in the total error,

TABLE II. Experimentally measured $B(E2)$ values in ^{109}Sn compared to $B(E2)$ values from shell-model (SM) calculations and predictions based on a simple core-excitation (CE) model with a ^{108}Sn core, $B(E2) = 0.222(19)$ e^2b^2 [7]. The SM values were used as starting values in the GOSIA2 analysis. For the $3/2^+$ states, both starting matrix elements tested in the analysis are given.

	$B(E2; 5/2_1^+ \rightarrow J_f)$	e^2b^2	
J_f	Exp	SM	CE
$3/2_2^+$	$0.029^{+0.014}_{-0.015}$	0.007 or 0.001	0.030(3)
$7/2_2^+$	$0.060^{+0.020}_{-0.022}$	0.047	0.060(5)
$9/2_1^+$	$0.085^{+0.032}_{-0.034}$	0.032	0.074(6)
$3/2_1^+$	$0.013^{+0.008}_{-0.011}$	0.001 or 0.007	0.030(3)
$5/2_2^+$	$<0.012^{\text{a}}$	0.004	0.044(4)
$1/2_2^+$	$<0.028^{\text{a}}$	0.008	0.015(1)

$^{\text{a}}$Measured $\chi^2 + 1$ upper limits.

treated as systematic deviations. In addition, the shell-model calculations discussed below predict that the $3/2_1^+$ level is the single-neutron state, at odds with the suggestions of β-decay measurements [15,16]. Therefore, we carried out an additional fit exchanging all relevant matrix elements related to these two states. This resulted only in a ~ 0.001 e^2b^2 decrease for the $B(E2)$ value of the $3/2_2^+$ state and a ~ 0.001 e^2b^2 increase of the $B(E2)$ value for the $3/2_1^+$ state. We have also investigated the effect of generating the $M1$ matrix elements using the effective neutron g factor, $g_s^{\text{eff}} = 0.7g_s$, instead of the values discussed below. No effects on the measured $B(E2)$ values were observed. Lastly, the possible presence of the $3/2_3^+ \rightarrow 5/2_1^+$ transition in Fig. 2 was estimated to decrease the $B(E2)$ value for the $7/2_2^+$ state by $\sim 10\%$. The effect was estimated based on the GOSIA2 predicted intensity using the shell-model calculated reduced matrix element for the $3/2_3^+$ state. This is accounted for in the uncertainty given in Table II.

The determined transition probabilities are compared to shell-model calculations and predictions of a simple core-excitation model in Table II. The shell-model calculations were carried out using a G-matrix renormalized charge-dependent (CD)-Bonn potential with the following set of single-neutron energies: $g_{7/2} = 0.0$ MeV, $d_{5/2} = 0.172$ MeV, $d_{3/2} = 2.1$ MeV, $s_{1/2} = 2.3$ MeV, and $h_{11/2} = 3.4$ MeV. The results for the calculated excited states are shown in the right side of Fig. 3 and give excellent agreement with the spin ordering and energies of the experimentally known states up to the $3/2_2^+$ level at 925 keV. The matrix elements were calculated using the standard neutron g factors, $g_l = 0$ and $g_s = -3.82$, and the neutron effective charge of $e_\nu = 1.0e$ [4].

The core-excitation model is based on the weak-coupling approach described in Ref. [17]. For the coupling of a neutron in the $d_{5/2}$ orbit to a 2^+ core state in a nearby even-even Sn nucleus, the model predicts a multiplet of states with $J \in 1/2^+, 3/2^+, 5/2^+, 7/2^+, 9/2^+$. The model predicts that the summed $B(E2 \uparrow)$ strength is equal to the $B(E2 \uparrow)$ value of the core state. The values given in Table II correspond to the $B(E2)$ strengths if the indicated state would be a part of the multiplet resulting from the coupling of a neutron to a ^{108}Sn 2^+ core.

The $B(E2)$ values of three of the higher lying states are well described within the framework of the core-excitation model. The data suggest that these states belong to a core-excitation multiplet. The missing members are then the $1/2^+$ and $5/2^+$ levels. Two low-lying $1/2^+$ states have been observed in ^{109}Sn. The lowest, at 545 keV, has been proposed to be the single-neutron state. The nonobservation of this level in the current measurement supports this assignment and suggests that the $1/2_2^+$ level belongs to the core-excitation multiplet. The $5/2_2^+$ state may be the missing $5/2^+$ member; however, its transition probability is largely overestimated by the core-excitation model. The shell-model gives a better description of the $E2$ properties of this state. Another possibility is that the $5/2^+$ multiplet member lies at a higher energy and was not directly excited in the experiment.

The $3/2_2^+$ state has been previously suggested to be the single-neutron state [15,16]. The state is strongly populated in the β decay of ^{109}Sb, similar to the heavier isotopes $^{111-117}$Sn [24]. The transition probabilities in Table II and shell-model calculations presented in this work, however, suggest that the $3/2_2^+$ state is a collective state. It may be that the strength of the collective excitation is distributed among both $3/2^+$ states. Interestingly, a low-lying $5/2^+$ state in ^{117}Sn, suggested to be a single-neutron state from nucleon-transfer reactions, was measured in Coulomb excitation to have a transition probability of ~ 6 W.u. [1]. The result was interpreted using the pairing-plus-quadrupole model and found to contain a large fraction of both the single-neutron and core-excited model states. A further consideration in ^{109}Sn arises from the small energy difference between the $d_{5/2}$ and $g_{7/2}$ neutron orbits. Consequently, the low-lying excited states may also contain a fraction of the $g_{7/2}$ core-coupled state.

Recently, we reported on the measurements of the reduced transition probability for the lowest $3/2^+$ state in ^{107}Sn [3]. This state lies 40 keV in energy above the $3/2_1^+$ state in ^{109}Sn, which suggests that they may have similar character. The measured $B(E2)$ value of $0.045^{+0.023}_{-0.017}$ e^2b^2 for the lowest $3/2^+$ state in ^{107}Sn is, however, ~ 3 times larger than the value for the $3/2_1^+$ state given in Table II. In ^{107}Sn, the proposed single-neutron state is at 1280 keV [16]. A possible explanation for the difference in the transition probabilities of the two low-lying $3/2^+$ states in these two nuclei is that the single-neutron state has moved up in energy in ^{107}Sn and is less mixed with the collective state. The collective strength is instead concentrated on the one $3/2^+$ state in ^{107}Sn as opposed to being distributed among the two $3/2^+$ states as in ^{109}Sn.

In conclusion, the measured transition probabilities can help to constrain the single-neutron energies relative to ^{100}Sn. As an example, consider the transition probability of the $3/2_2^+$ state. As was discussed in Ref. [3], the inversion of the $g_{7/2}$ and $d_{5/2}$ orbits generally leads to a decrease in the calculated collectivity of the state. This effect can be compensated for by adjusting the energies of the three higher lying single-neutron orbits. The trend is that lowering the energy of $d_{3/2}$ state decreases the collectivity, while the opposite is true for the $s_{1/2}$ and $h_{11/2}$ orbits. However, the energy of the $h_{11/2}$ state is also constrained experimentally by the energies of the first

$11/2^-$ states in ^{107,109}Sn. In the case discussed here, the measurements indicate that neither of the observed $3/2^+$ states is a $d_{3/2}$ single-neutron state. The population of the $3/2_2^+$ state would not be expected if it was a pure single-neutron state, particularly since it lies ~ 300 keV higher than the $3/2_1^+$ state. This observation effects the possibility of using the $3/2^+$ states in ^{109}Sn to constrain the energy of the $d_{3/2}$ orbit. On the other hand, the fact that we did not observe excitation of the 545-keV state strengthens the $1/2^+$ assignment of this state. It should also be mentioned that the shell-model calculations presented in this work do not include excitations across the $N = Z = 50$ closed proton and neutron shells. These missing excitations may increase the collectivity of the shell-model calculations; see Refs. [4–7].

We have presented the first Coulomb excitation measurement of the radioactive isotope ^{109}Sn. A set of reduced transition probabilities for the observed excited states were deduced using the semi-classical Coulomb excitation code GOSIA2. The results indicate that a significant quadrupole strength exists in the low-lying excited states and thus highlight the importance of both single-neutron and collective excitations near the doubly magic nucleus ^{100}Sn.

[1] P. H. Stelson *et al.*, Nucl. Phys. A **190**, 197 (1972).
[2] W. K. Dagenhart *et al.*, Nucl. Phys. A **284**, 484 (1977).
[3] D. D. DiJulio *et al.*, Eur. Phys. J. A **48**, 105 (2012).
[4] A. Banu *et al.*, Phys. Rev. C **72**, 061305(R) (2005).
[5] J. Cederkäll *et al.*, Phys. Rev. Lett. **98**, 172501 (2007).
[6] C. Vaman *et al.*, Phys. Rev. Lett. **99**, 162501 (2007).
[7] A. Ekström *et al.*, Phys. Rev. Lett. **101**, 012502 (2008).
[8] BNL Evaluated Nuclear Structure Data File (ENSDF), http://www.nndc.bnl.gov/ensdf/.
[9] J. Blachot, Nucl. Data Sheets **110**, 1239 (2009).
[10] D. Seweryniak *et al.*, Phys. Rev. Lett. **99**, 022504 (2007).
[11] I. G. Darby *et al.*, Phys. Rev. Lett. **105**, 162502 (2010).
[12] C. Fahlander *et al.*, Phys. Rev. C **63**, 021307(R) (2001).
[13] J. Eberz *et al.*, Nucl. Phys. A **464**, 9 (1987).
[14] L. Kaubler *et al.*, Z. Phys. A **351**, 123 (1995).
[15] I. Dankó *et al.*, Nucl. Phys. A **646**, 3 (1999).
[16] J. J. Ressler *et al.*, Phys. Rev. C **65**, 044330 (2002).
[17] A. de Shalit, Phys. Rev. **122**, 1530 (1961).
[18] V. Fedoseyev *et al.*, Hyp. Int. **127**, 409 (2000).
[19] A. N. Ostrowski *et al.*, Nucl. Instrum. Methods Phys. Res. A **480**, 448 (2002).
[20] P. Reiter *et al.*, Nucl. Phys. A **701**, 209 (2002).
[21] C. D. Nesaraja *et al.*, Nucl. Data Sheets **111**, 897 (2010).
[22] J. Blachot, Nucl. Data Sheets **107**, 355 (2006).
[23] T. Czosnyka *et al.*, Bull. Am. Phys. Soc. **28**, 745 (1983).
[24] M. E. J. Wigmans *et al.*, Phys. Rev. C **14**, 229 (1976).